

# Low-Profile Microstrip Antenna with Bandwidth Enhancement for RFID Applications

Peng Yang, Shiquan He, Yan Li and Lijun Jiang

Peng Yang, Shiquan He and Yan Li are with School of Electronic Engineering, University of Electronic Science and Technology of China (UESTC), Chengdu, China. (e-mail: [yangp001@tom.com](mailto:yangp001@tom.com), [yangpeng@ee.uestc.edu.cn](mailto:yangpeng@ee.uestc.edu.cn)). Lijun Jiang is with the University of Hong Kong, Hong Kong.

*Abstract*— Two low-profile microstrip antennas, which can be mounted on metallic objects for RFID applications, are proposed. By using a single layer FR4 as the substrate, the thickness of the antennas is only 1.6 mm (about 1% dielectric wavelength at 900 MHz). In order to broaden the bandwidth, slots are added on the surface of the patch to excite two different modes. Compared to conventional microstrip antennas, the impedance bandwidth ( $VSWR < 3$ ) of the design can reach 100 MHz and the 3 dB gain bandwidth is about 50 MHz, which can satisfy most applications for UHF RFID system. The size of the compact design is only 84 mm  $\times$  26 mm. Prototypes were fabricated and measured. The read range of the designed antennas can reach 4 meters when mounted on metallic plates.

*Index Terms*—Low profile, broadband, microstrip antenna, RFID tag, platform-tolerant

## I. INTRODUCTION

Radio frequency identification (RFID) is one of the recently growing technologies for wireless identification [1]. The tag antenna design is one of the key techniques in RFID systems [2]. To lower the tag cost, most antennas are printed on paper using the conductive ink. Usually, these antennas are of dipole-type structures. They perform well when they are put in air or mounted on dielectrics such as wood or plastics. However, they are very sensitive to the environment and do not work when they are on metal surfaces or liquid containers due to the image theory [3].

The microstrip antenna is a good choice for platform-tolerant RFID tags because of the ground plane in its structure. However, it is well known that the biggest shortcoming of microstrip antennas is the narrow bandwidth due to its resonant structure with a high Q factor. The situation becomes even worse when the thickness of the antenna becomes very thin. For a typical microstrip antenna with a thickness about 1% of wavelength in free space, its fractional bandwidth is no more than 2%, which is not enough for broadband RFID applications. Hence, a challenging issue in the microstrip RFID tag antenna design is on how to broaden the tag antenna's

bandwidth while keeping its low-profile characteristics.

Various approaches have been presented in the literature for the low-profile platform-tolerant RFID tag design. For example, one can design a loop feed with two short stubs and two symmetrical radiating patches shorted to ground [4]. This antenna has a fractional impedance bandwidth of 8% ( $VSWR < 3$ ) in air, but the VSWR becomes poor when mounted on a metallic surface. In [5], by embedding a pair of U-shaped narrow slots close to the non-radiating edges of a rectangular microstrip patch, two modes can be excited. This antenna has a 14.5% bandwidth. However, the gain of this antenna has a large variation in the whole impedance bandwidth. In [6], a double-resonance bow-tie patch antenna with a microstrip feed was proposed. Though this antenna has two resonant frequencies, its available bandwidth is only 20 MHz. In [7], a compact structure using two shorted patches and an inductively coupled feed was developed to achieve a good performance even when it is attached to metallic objects. But its bandwidth is not wide enough to cover the band of North America (902 MHz to 928 MHz). Moreover, the thickness of this antenna is 3 mm. It seems too thick for RFID tag applications. Recently, there are some low-profile, broadband microstrip antenna designs for UHF RFID. In [8], two parasitic patches are put close to the non-radiating edge of the main patch for the bandwidth enhancement. The bandwidth ( $S_{11} < -7\text{dB}$ ) of this design is about 120 MHz. However, it is not compact enough because the parasitic patches occupy additional spaces. In [9], a T-shaped microstrip line is added at one of the radiating edges of a rectangular patch to obtain a dual-resonance. The occurrence of the two resonant modes is mainly due to the integrated reactive loading which provides a capacitive load at the lower resonant frequency and an inductive load at the higher resonant frequency. The shortcoming of this design is that its size is still too big (98 mm  $\times$  50 mm). In [10], the antenna is composed of four synchronous shorted patches that resonate at four different frequencies, broadening its impedance bandwidth. However, the antenna is not easy for fabrication because there are four via holes in the structure.

In this paper, two kinds of low-profile microstrip antennas with bandwidth enhancement are proposed. By adding slots on the patch surface, two different resonant modes can be excited. The antenna is compact enough while keeping low-profile and broadband characteristics. The impedance bandwidth ( $VSWR < 3$ ) of the antenna can be over 10% and 3dB gain bandwidth is about 5%.

## II. ANTENNA DESCRIPTION

Several methods can be used for the bandwidth enhancement of microstrip antennas. One effective way is to use the thick substrate with low permittivity. However, for RFID tag antennas, it is critical to maintain the

low-profile characteristic. Another approach is to use multi-patches with different sizes so that they can resonate at different frequencies. But its size is also large. An effective way for the single-layer, single-patch bandwidth enhancement is to excite multi-modes by changing the structure of the patch. Each mode resonates at a different frequency. If these frequencies can be adjusted to be close to each other, wide bandwidth can be achieved. For example, a fractional bandwidth over 30% has been obtained by using an E-shape or a U-slot loaded patch antenna [11], [12].

Fig. 1 shows the geometry and the parameters of the proposed antenna. The size of the patch is 76 mm  $\times$  60 mm. The dielectric between the patch and the ground is FR4 with permittivity 4.3, and loss tangent 0.02. The thickness  $h$  of the FR4 is 1.6 mm. Unlike conventional 50 ohms microstrip antenna, the imaginary part of the RFID tag's impedance has to be inductive at resonant frequency to conjugate match to the capacitive RFID chip. A shorted microstrip line with length  $L_f$  and width  $W_f$  is used to provide such inductive impedance. By changing the length and width of the microstrip line, the desired inductance can be obtained [13].

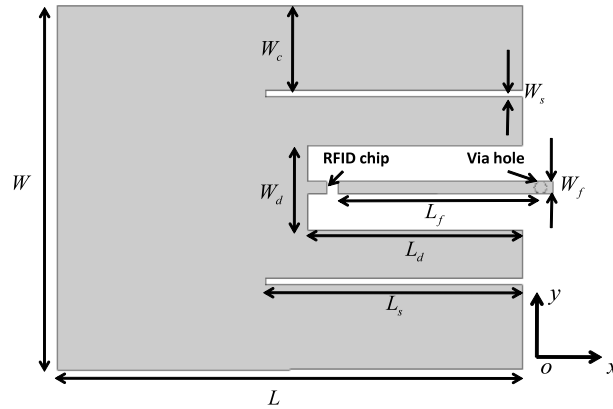


Fig. 1. The geometry of the two-slot antenna. Where  $L = 76$ ,  $W = 60$ ,  $L_d = 35$ ,  $L_s = 42$ ,  $W_s = 1$ ,  $L_f = 33$ ,  $W_f = 2$ ,  $W_c = 14$  and  $W_d = 14$ . All units are in mm.

The bandwidth of a microstrip antenna with the same thickness at 900 MHz is not more than 3%. To broaden its bandwidth, a pair of thin slots with width  $W_s$  and length  $L_s$  is cut from one radiation edge to the center of the patch to yield two modes resonating at different frequencies. Fig. 2 shows the two resonant modes. The first mode is the normal  $TM_{10}$  mode; all of the currents on the surface of the patch flow from point  $A$  to point  $B$  (Fig. 2(a)). The length of the slot is chosen a little bit longer than half length of the patch. Hence, if the frequency is lower than that of the first mode, the currents close to the slots will flow around it (i.e. from point  $A$  to point  $C$ , Fig.2(c)). The currents far away from the slots (those close to the edge of the patch) will keep flowing from point  $A$  to point  $B$ , the same as the first mode. Hence, for the second mode, by changing the

width  $W_c$ , we can adjust the currents ratio to determine how much currents flow from  $A$  to  $B$  and how much from  $A$  to  $C$ . The currents flow from  $A$  to  $C$  have opposite directions, and therefore have little contribution to the radiation. Hence, if the antenna is resonating well at the second mode, the gain will be lower than the first mode. Therefore, the gain bandwidth would be narrower than the impedance bandwidth. There is a trade-off between the impedance bandwidth and the gain.

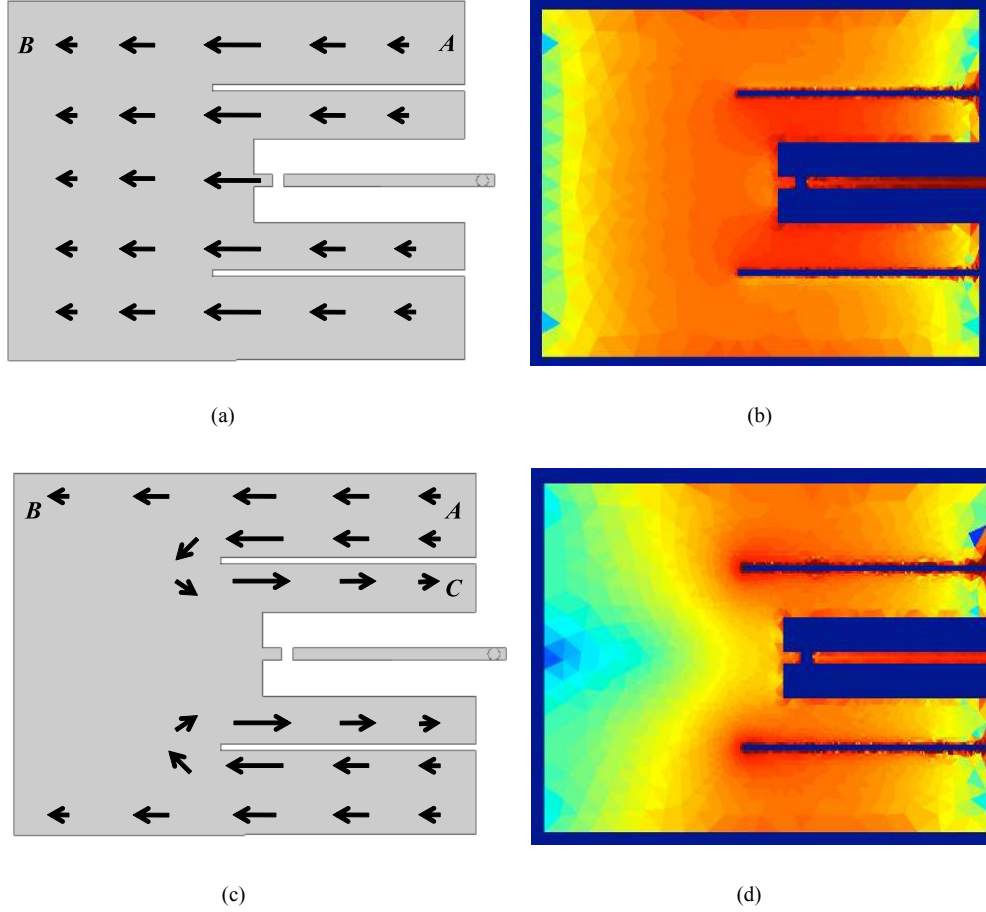


Fig. 2. Current distribution of two modes. (a) Vector current of the first mode. (b) Current magnitude of the first mode. (c) Vector current of the second mode. (d) Current magnitude of the second mode.

From a circuit model perspective, the microstrip antenna with multi-mode can be represented by parallel  $RLC$  networks.

$$Z_{in} = \sum_{i=0}^{\infty} \frac{1}{G_i(\omega) + j\omega C_i + 1/(j\omega L_i)} \quad (1)$$

It is easy to determine the values of  $G_1$ ,  $L_1$  and  $C_1$  of the first mode ( $TM_{10}$ ) by using the cavity model theory [14]. For the second mode, there is a convenience way. When two slots are incorporated into the patch, some of the currents will flow around the slots; the length of the current path will increase. This effect is equal to an additional serial inductance  $\Delta L$  [11]. Hence, the effective inductance  $L_2$  should be larger than  $L_1$ , which

makes the resonant frequency of mode 2 lower than mode 1. More details about the effects of the slots and the calculation of parameters of mode 2 can be found in reference [15].

The shorted microstrip line creates a shorted  $\lambda/4$  resonator. Hence, it can also be modeled by a parallel  $RLC$  circuit [16]. The equivalent resistance and capacitance are:

$$\begin{cases} R_s = Z_0 / \alpha L_f \\ C_s = \pi / 4\omega_0 Z_0 \end{cases} \quad (2)$$

where  $\alpha$  is the attenuation constant,  $Z_0$  is the characteristic impedance of the microstrip line, and  $\omega_0$  is the resonant frequency of the shorted  $\lambda/4$  resonator. The inductance  $L_s$  can be calculated by  $L_s = 1/(\omega_0^2 C_s)$ . The step change in the width of the microstrip line to the patch can be modeled by a shunt inductance  $L_c$  and a series capacitance  $C_c$ . These two parameters are not easy to calculate but they can be extracted through the numerical or experiment results. The resonant frequencies of this antenna are determined by the patch length and the slots. The input impedance can be adjusted by changing the length, and width of the shorted microstrip line, as well as the location of the RFID chip on the microstrip line. The final equivalent circuit model of this antenna is shown in Fig. 3.

To evaluate the performance of the design, we use a FEM-GIBC (finite element - general impedance boundary condition method) based code [16] to do the full wave simulation. The simulated input impedance by the full wave solver and the circuit model are shown in Fig. 4. Two resonant modes can be seen clearly. After some tuning, the results of the two methods can match well with each other. The scalar current distributions on the surface of the patch are shown in Fig. 2(b) and Fig. 2(d) at 870 MHz and 960 MHz, respectively.

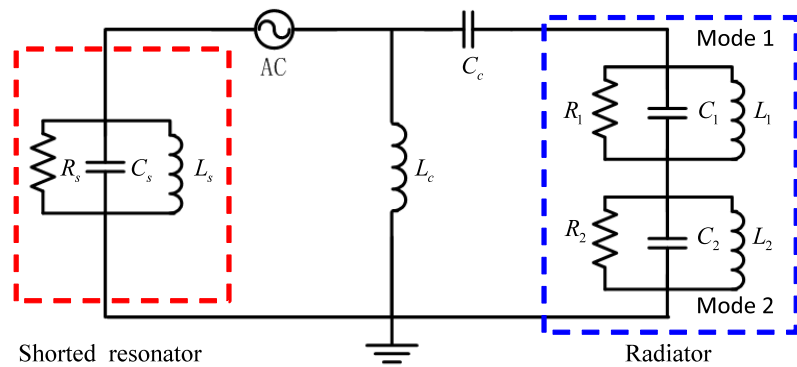


Fig. 3. The equivalent circuit of the proposed two-slot antenna, where  $R_1 = 450 \text{ ohm}$ ,  $R_2 = 300 \text{ ohm}$ ,  $C_1 = 24.1 \text{ pF}$ ,  $C_2 = 20.2 \text{ pF}$ ,  $L_1 = 1.1 \text{ nH}$ ,  $L_2 = 1.54 \text{ nH}$ ,  $R_s = 3500 \text{ ohm}$ ,  $C_s = 1.4 \text{ pF}$ ,  $L_s = 9 \text{ nH}$ ,  $C_c = 0.9 \text{ pF}$ ,  $L_c = 8.9 \text{ nH}$ .

Though the two-slot structure has two modes on the single patch, its size seems too large ( $76 \text{ mm} \times 60 \text{ mm}$ ) to be a tag antenna. Because the antenna discussed above has a symmetrical structure, the cross section ( $xz$

plane) of the antenna can be seen as a perfect magnetic conductive (PMC) wall. Hence, it is possible to split the antenna along  $xz$  plane at the center of the patch to reduce the total size. Fig. 5 shows the geometry and parameters of the improved single-slot antenna. It can be seen that the size of the patch has a significant reduction. Note that the single-slot antenna is not simply one half of the double-slot antenna. When the double-slot antenna is split along the  $xz$  plane, the widths of the patch and the shorted line are changed. Also, the impedance of the antenna will be changed. However, the working principles of these two antennas are the same. Hence, the single-slot antenna has the same circuit model as the double-slot one shown in Fig. 3. Of course, the values of the lumped elements should be different.

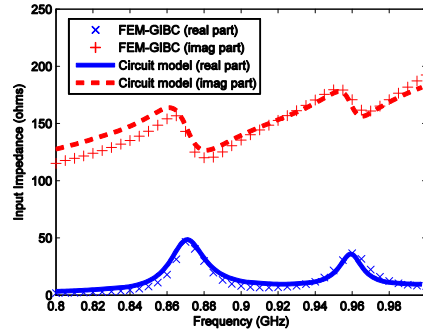


Fig. 4. Simulated input impedance of the proposed two-slot antenna. (Solid line: FEM-GIBC. Dots: Circuit model.)

### III. PROTOTYPES AND MEASUREMENTS

To prove the performance of this design, prototypes were fabricated and measured. Fig. 6 shows the prototypes of these two kinds of antennas. With the method proposed by [17], the input impedance of these antennas are measured by using an Agilent 8753ES two port vector network analyzer. Fig. 7 shows the measured input impedance and VSWR. The two-slot antenna is designed for Alien's Higgs-2 RFID chip while the single-slot is for Higgs-3 chip. The impedances of these two chips at different frequencies are also plotted in Fig. 7 with dash lines. From Fig. 7, it is seen that the bandwidths of the antennas are broadened by introducing two resonant modes. The impedance bandwidth of the two-slot antenna ( $VSWR < 3$ ) is from 850 MHz to 940 MHz while the single-slot is from 845 MHz to 950 MHz. However, the gain bandwidth of the antennas are narrower than the impedance bandwidth. The reason is mentioned in Section II. The simulated broadside realized gain and radiation patterns of these two antennas when mounted on metallic plate are shown in Fig. 8. For the two-slot antenna, the maximum gain is about  $-1.5$  dB, and the 3 dB gain bandwidth is around 80 MHz (from 880 MHz

to 960 MHz). For single-slot antenna, the maximum gain is about  $-3$  dB, and 3dB gain bandwidth is 50 MHz (from 880 MHz to 930 MHz). The low gain is due to the thin thickness of the structure and the high loss of the substrate FR4 we used ( $\epsilon_r = 4.2, \tan \delta = 0.02$ ).

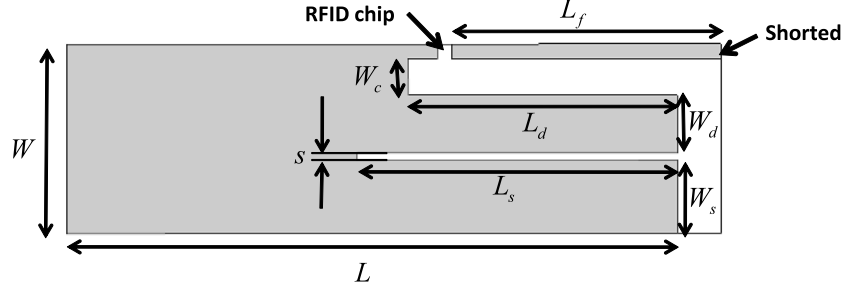
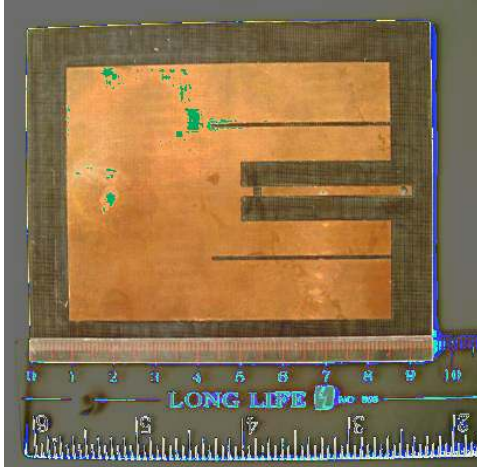
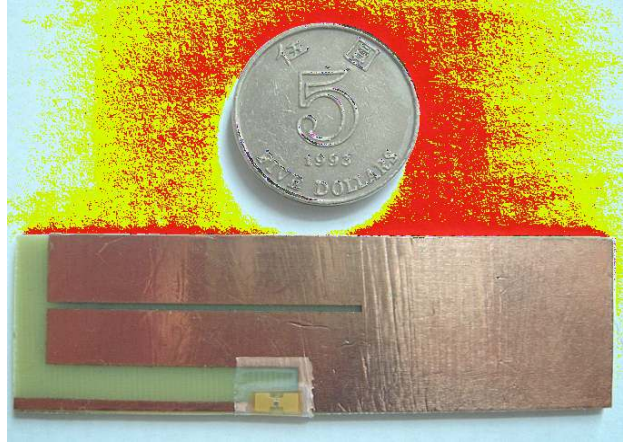


Fig. 5. Geometry of the single-slot antenna, where  $L = 84$ ,  $L_s = 44$ ,  $L_d = 37$ ,  $L_f = 37$ ,  $W = 26$ ,  $W_s = 10$ ,  $W_d = 8$ ,  $W_c = 5$ ,  $s = 1$ . All units are in mm.



(a)



(b)

Fig. 6. Prototypes of the proposed tags. (a) Two-slot antenna. (b) Single-slot antenna.

The read ranges of the proposed RFID tag antennas are measured by using the Impinj Speedway reader. The total output power is fixed to 30 dBm and the operating frequency hops from 900 MHz to 930 MHz (the performance of the antennas within the whole bandwidth cannot be measured due to the limit of the reader). The results are shown in Table I. From the measurement results, we found that the read range has a significant enhancement for the single-slot antenna when mounted on metallic surface. But the enhancement is very limited for the two-slot antenna. This is because the two-slot antenna has a relatively larger ground size itself than the single-slot antenna. The maximum read range of the two antennas is almost same: about 4 meters. This is because the Higgs-3 chip used for the single-slot antenna is more sensitive than Higgs-2 chip for the two-slot antenna.

#### IV. CONCLUSIONS

In this work, two types of low-profile microstrip tag antennas with bandwidth enhancement for RFID applications are proposed. By adding slots on the patch, two different modes can be excited. These two modes resonate at different frequencies to enable the broad bandwidth. The size of the compact design (single-slot antenna) is only  $84 \text{ mm} \times 26 \text{ mm} \times 1.6 \text{ mm}$  with an impedance bandwidth over 100 MHz ( $\text{VSWR} < 3$ ), and 3dB gain bandwidth of 50 MHz. A four meter read range is achieved when it is put on metallic object. The compact size and the concise design make this type of antennas very easy to fabricate and suitable for low cost RFID applications.

#### V. ACKNOWLEDGMENT

This work was supported in part by Innovation and Technology Fund (ITF, No. ITS/159/09 and No. ITS/347/09), the government of the Hong Kong SAR Hong Kong, and in part by Hong Kong R & D Centre for Logistics and Supply Chain Management Enabling Technologies (LSCM).

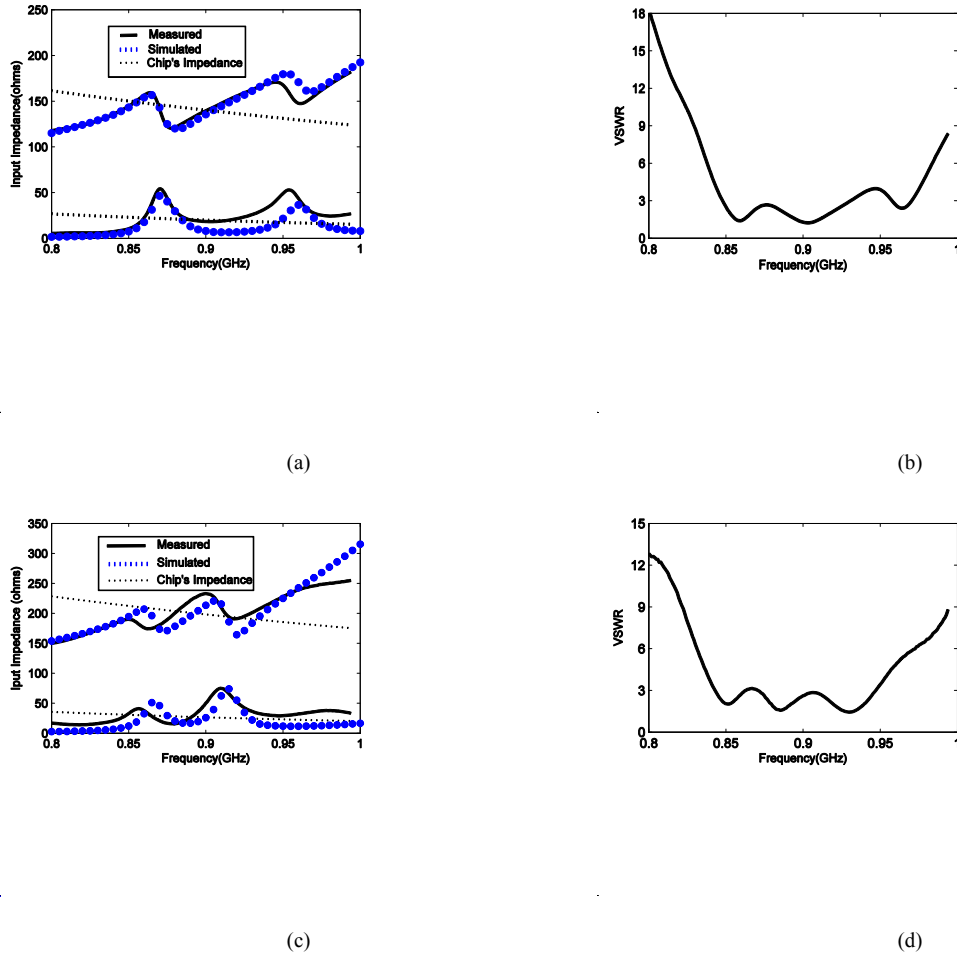
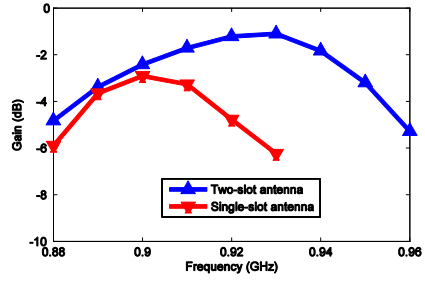
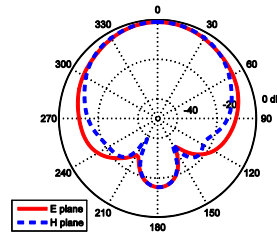
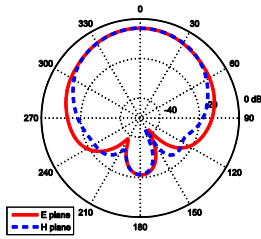


Fig. 7. Simulated, measured input impedance and VSWR. (a) Input impedance of the two-slot antenna. (b) VSWR of the two-slot antenna. (c) Input impedance of the single-slot antenna. (d) VSWR of the single-slot antenna.

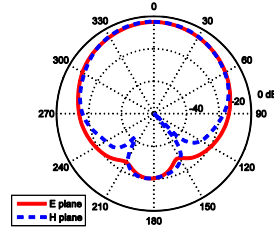
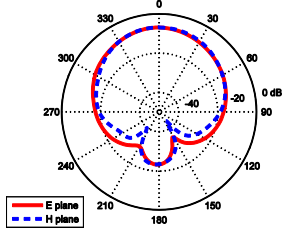




(a)



(b)



(c)

Fig. 8. Simulated realized gain and radiation patterns. (a) Simulated realized gain. (b) Radiation patterns of double-slot antenna at 880 MHz and 930MHz. (c) Radiation patterns of single-slot antenna at 880 MHz and 910MHz.

TABLE I  
READ RANGE OF THE PROPOSED ANTENNAS

	TOW-SLOT ANTENNA	SINGLE-SLOT ANTENNA
Free Space	3.7 m	2.5 m
Metallic Plate	4.2 m	4 m

## REFERENCES

- [1] D. M. Dobkin. 2008. *The RF in RFID: Passive UHF RFID in Practice*, Elsevier Inc, Burlington. MA,.
- [2] G. Marrocco. 2008. The art of UHF RFID antenna design: Impedance matching and size reduction techniques. *IEEE Antennas Propag. Mag.*, vol. 50(1), pp. 66-79.
- [3] C. A. Balanis, *Antenna Theory: Analysis and Design*. John Wiley & Sons, New York, 2005.
- [4] Q. Z. Chen and B. J. Hu. 2008. Novel UHF RFID tag antenna with shorted stubs mountable on the metallic objects. *Int. Conf. Microw. Millim. Wave Technol.*, vol. 4, pp. 1822-1824.
- [5] L. Mo, H. Zhang and H. Zhou. 2008. Broadband UHF RFID tag antenna with a pair of U slots mountable on metallic objects, *Electron. Lett.*, vol. 44(20), pp. 1173-1174.
- [6] J. Dacuna and R. Pous. 2009. Low-profile patch antenna for RF identification applications. *IEEE Trans. Microw. Theory Tech.*, vol. 57(5), pp. 1406-1410.
- [7] B. Yu, S. J. Kim and B. Jung. 2007. RFID tag antenna using two-shortened microstrip patches mountable on metallic objects. *Microw. Opt. Technol. Lett.*, vol. 49(2), pp. 414-416.
- [8] M. Y. Lai, R. L. Li and M. M. Tentzeris. 2010. Low-profile broadband RFID tag antennas mountable on metallic objects. *IEEE AP-S Int. Symp.* pp.1-4.
- [9] M. Y. Lai and R. L. Li. 2010. A low-profile broadband RFID tag antenna for metallic objects. *IEEE AP-S Int. Symp.*, pp. 1891-1893.
- [10] J. Zh. Huang, P. H. Yang, W. C. Chew and T. Ye. 2010. A novel broadband patch antenna for universal UHF RFID tags. *Microw. Opt. Technol. Lett.*, vol. 52(12), pp. 2653-2657.
- [11] F. Yang, X. X. Zhang, X. Ye and Y. Rahmat-Samii. 2001. Wide-band E-shaped patch antennas for wireless communications. *IEEE Trans. Antennas Propag.*, vol. 49(7), pp. 1049-1100.
- [12] T. Huynh and K. F. Lee. 1995. Single layer single patch wideband microstrip antenna. *Electron. Lett.*, vol. 31(16), pp. 1310-1312.
- [13] L. F. Mo and C. F. Qin. 2010. Planar UHF RFID tag antenna with open stub feed for metallic objects. *IEEE Trans. Antennas Propag.*, vol. 58(9), pp. 3037-3043.
- [14] W. F. Richards, Y. T. Lo and D. D. Harrison. 1981. An improved theory for microstrip antennas and applications. *IEEE Trans. Antennas Propag.*, vol. 29(1), pp. 38-46.
- [15] X. X. Zhang and F. Yang. 1998. The study of slit cut on the microstrip antenna and its applications,. *Microwave Opt. Technol. Lett.*, vol. 18(4), pp.297-300.
- [16] D. M. Pozar. 2005. *Microwave Engineering*, Third Edition, John Wiley & Sons, New York.
- [17] K. D. Palmer and M.W. van Rooyen. 2006. Simple broadband measurements of balanced loads using a network analyzer. *IEEE Trans. Instrum. Meas.*, vol. 55(1), pp. 266-272.